Landau levels and persistent currents in nonuniform magnetic fields

Chang Sub Kim and Oleg Olendski
Department of Physics, Chonnam National University, Kwangju 500-757, Korea
(Received 21 November 1995; revised manuscript received 10 January 1996)

The single-particle energy spectra are calculated for a two-dimensional electron gas under perpendicularly applied nonuniform magnetic fields. It is found that the spatial modulation of magnetic fields in an annular geometry can lift the degeneracy of bulk Landau levels, and accordingly results in current-carrying states that are distinguished from the edge states. The prominent features of the calculated energy spectrum are anticrossing and the repulsion of levels. The net current does not vanish in the ground state due to the presence of the lower-lying current-carrying states below the Fermi energy. Quantum structures confined by electrostatic potential barriers are also investigated within an independent electron approximation. Consequently, a rich structure of persistent currents is obtained at zero temperature as a function of the electron number and magnetic field variation.

I. INTRODUCTION

When a uniform magnetic field is applied perpendicularly to an unbounded two-dimensional ideal electron gas, the Landau levels emerge with infinite degeneracy.[1] On the other hand, in a realistic situation a system is typically bounded, and so the density of each Landau level becomes finite. It can be estimated that the density of states is proportional to the magnetic field, which results in such interesting physics as the Shubnikov–de Haas effect.[2] It has been shown that the degeneracy of the Landau levels is lifted near a barrier that may represent a conduction band discontinuity, where the magnetic field is applied in the plane of interest.[3,4] This lift of degeneracy gives rise to the interesting anticrossing and repulsion of levels in the energy spectrum that have recently been extensively investigated.[5–10] The pronounced features of the anticrossing and level repulsion can also be achieved by perturbing the applied magnetic fields. By applying spatially modulated magnetic fields perpendicular to the interface, interesting electronic and transport properties such as the oscillatory magnetoresistivity have been predicted theoretically[11–15] and observed experimentally.[16–20]

The Landau levels can be labeled by the radial quantum number n and the magnetic index m in the direction of the applied fields when a cylindrical geometry is considered. For $m \leqslant 0$ all levels are degenerate for a given n, and thus m plays a role similar to the guiding center of magnetic oscillation in Cartesian geometry. What is important is that none of these levels carries current except the $m=0$ level. The levels with positive m for a given n carry current. However, they can be reinterpreted as belonging to a higher level with $n \rightarrow n+i$, where $i \geqslant 1$. Thus, the equilibrium current vanishes for such a system, which may exclude the $m=0$ orbital because there are infinitely many non-current-carrying orbits to be filled by electrons in the ground state, which all possess the same lowest energy. In other words, the Fermi energy is locked on the lowest energy level. On the other hand, the current-carrying levels can be lifted by imposing rigid wall boundary conditions. Recently, persistent currents have been calculated and analyzed for an annulus quantum ring, as well as a quantum disk where essentially the edge states near the hard wall boundaries enabled the nonvanishing current.[21,22] Also, a magnetically confined electron in a nonuniform magnetic field has been studied in inverse Aharonov-Bohm arrangements, where attention was paid mainly to the energy eigenvalues compared to the Landau levels, not including the associated currents.[23]

Since the degeneracy of Landau levels can be lifted by a spatial modulation of applied magnetic fields it seems to be a worthwhile endeavor to investigate a simple theoretical model that may generate current-carrying levels inside bulk. In this work we propose a simple quantum structure that enables us to study in detail the lift of the degeneracy of bulk Landau levels and consequently to understand its effect on the persistent currents in a quantum disk. We will present an exact numerical solution for the single-particle energy spectrum by solving the relevant Schrödinger equation and the resulting persistent current within an effective-mass approximation. We hope that our model calculation may bring insight to the comprehension of magnetotransport on a smaller length scale than the average electron mean free path.

The model we consider is described here briefly. We first take an electron gas confined in one direction and assume that an external magnetic field is applied perpendicular to the interface, not uniformly but in a spatially modulated way. The plane polar geometry is taken so that the magnetic fields are perturbed in an annulus shape. Our results show that this simple geometrical perturbation of applied magnetic fields induces rich structures in the energy spectrum, such as anticrossing and the repulsion of levels. Also, it is seen that the degeneracy of Landau levels is lifted in the bulk, which results in current-carrying states. Subsequently, the net equilibrium currents are evaluated at zero temperature for a wide range of the applied magnetic fields as a function of the electron number. Although the Fermi energy is locked on the ground orbit of $n=0$, the total current does not vanish, and instead, manifests an interesting structure. Next, quantum disk problems are considered by introducing an outer barrier (both a soft wall and a hard wall) at the distance D from the origin in the limit of high magnetic field, $D \gg r_B$ where r_B is the magnetic length. In this case, the edge states emerge and play a crucial role in determining the Fermi energy, which

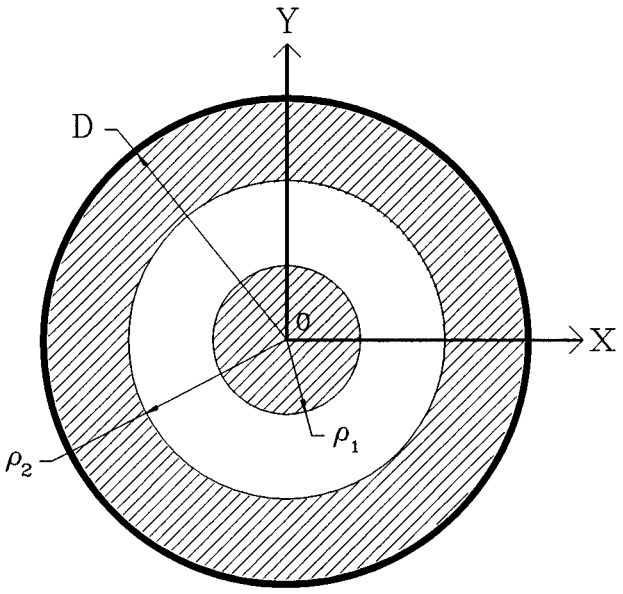

FIG. 1. Quantum structure considered: spatially modulated nonuniform magnetic fields are applied perpendicularly to a quantum disk of radius D where a field-free annulus with inner radius ρ_1 and outer radius ρ_2 is introduced.

can be locked at a higher Landau level $n>0$. The resulting persistent current becomes more intriguing. Finally, it is emphasized that our results have been obtained by exactly solving the relevant Schrödinger equation instead of expanding wave functions in the plane-wave basis as is done in.[21]

In Sec. II the model we consider is described and the necessary theoretical formulation is also given. The results are presented in Sec. III with discussions. Finally, concluding remarks are provided in Sec. IV. We have included the transcendental equation that determines the energy spectrum in the Appendix.

II. MODEL AND FORMULATION

We consider a two-dimensional spinless electron gas in the presence of magnetic fields applied perpendicular to the system. Instead of applying the fields uniformly over all space we modulate them spatially such that a field-free annulus with an inner radius ρ_1 and an outer radius ρ_2 is surrounded by an otherwise uniform magnetic field $\vec{B}=(0,0,B)$. In addition, we introduce into our model a potential barrier of the form

$$V(\rho)=\begin{cases} 0, & \rho\leqslant D \\ V_0, & \rho\geqslant D, \end{cases} \tag{1}$$

in order to incorporate the problem of a quantum disk, where D is the radius of disk. Our model structure is depicted schematically in Fig. 1.

Within an independent electron approximation the single-particle energy spectrum is determined by solving the Schrödinger equation of the form ($c\equiv 1$)

$$\left\{\frac{1}{2m_e^*}(\vec{p}+e\vec{A})^2+V(\rho)\right\}\Psi(\rho,\varphi)=E\Psi(\rho,\varphi), \tag{2}$$

where e is the absolute value of the charge of an electron, m_e^* is the effective mass of the electron, E is the energy eigenvalue, and $\vec{A}$ is the relevant vector potential to be specified. In the plane polar coordinates $\vec{r}=(\rho,\varphi)$ the vector potential can be specified by choosing the symmetric gauge

$$A_\varphi(\rho)=\begin{cases} \dfrac{1}{2}B\rho, & \rho\leqslant\rho_1 \\ \dfrac{1}{2}B\dfrac{\rho_1^2}{\rho}, & \rho_1\leqslant\rho\leqslant\rho_2 \\ \dfrac{1}{2}B\rho\left(1-\dfrac{\rho_2^2-\rho_1^2}{\rho^2}\right), & \rho\geqslant\rho_2. \end{cases} \tag{3}$$

After substituting the vector potential into Eq. (2) with an ansatz for the wave function of the form

$$\Psi(\rho,\varphi)=\frac{1}{\sqrt{2\pi}}R(\rho)\exp(im\varphi), \tag{4}$$

where m is an integer, one can separate out the equations for the radial wave function. Here, one should notice that m is not the eigenvalue of the angular momentum operator in the current situation where the magnetic field is present. It simply labels the angular momentum states and hereafter it will be called the magnetic index.

The solutions to the radial part of the Hamiltonian can be obtained in terms of Bessel functions $J_\nu(x)$ and $Y_\nu(x)$ in the field-free region, and confluent hypergeometric functions $M(a,b,x)$ and $U(a,b,x)$ in the regions where magnetic fields are present (see Ref. 24 for notations). For instance, in the domain $\rho_2\leqslant\rho\leqslant D$, the result is given as

$$R(\rho)=\exp\left(-\frac{1}{4}\frac{\rho^2}{r_B^2}\right)\left(\frac{1}{2}\frac{\rho^2}{r_B^2}\right)^\gamma\left\{A_4U\left(\alpha-\frac{E}{\hbar\omega_B},\beta,\frac{1}{2}\frac{\rho^2}{r_B^2}\right)+A_5M\left(\alpha-\frac{E}{\hbar\omega_B},\beta,\frac{1}{2}\frac{\rho^2}{r_B^2}\right)\right\}. \tag{5}$$

In the above $r_B=(\hbar/eB)^{1/2}$ is the magnetic radius, $\omega_B=eB/m_e^*$ is the cyclotron frequency, and the following definitions have been made:

$$\alpha=\frac{1}{4}\left\{2+2m-\left(\frac{\rho_2^2}{r_B^2}-\frac{\rho_1^2}{r_B^2}\right)+\left|2m-\left(\frac{\rho_2^2}{r_B^2}-\frac{\rho_1^2}{r_B^2}\right)\right|\right\}, \tag{6}$$

$$\beta=1+\frac{1}{2}\left\{\left|2m-\left(\frac{\rho_2^2}{r_B^2}-\frac{\rho_1^2}{r_B^2}\right)\right|\right\}, \tag{7}$$

$$\gamma=\frac{1}{4}\left\{\left|2m-\left(\frac{\rho_2^2}{r_B^2}-\frac{\rho_1^2}{r_B^2}\right)\right|\right\}. \tag{8}$$

Throughout this paper we will use the dimensionless energy E^* and barrier height V_0^*, expressed in units of $\hbar\omega_B$ as

$$E^*\equiv\frac{E}{\hbar\omega_B}, \quad V_0^*\equiv\frac{V_0}{\hbar\omega_B}. \tag{9}$$

The coefficients A_i that appear in radial equations are specified by the continuity of the wave functions and their

derivatives at each boundary, and the normalization condition $\int_0^\infty R^2(\rho)\rho d\rho = 1$. These matching conditions give rise to a set of linear homogeneous algebraic equations. The requirement of vanishing for the determinant of this linear system for a nontrivial solution results in the transcendental equation, which is given in the Appendix. The obtained transcendental equation determines the energy eigenvalues E^*_{nm}, with n being the radial quantum number.

Once the wave functions are determined, one can calculate the associated currents. The current density carried by the state Ψ_{nm} can be obtained from[25]

$$\vec{j}_{nm}(\rho,\varphi) = -\left[\frac{e\hbar}{m_e^*}\mathrm{Im}(\Psi^*\nabla\Psi) + \frac{e^2}{m_e^*}\vec{A}\Psi^*\Psi\right]. \quad (10)$$

In the present investigation only the azimuthal component of the current density is relevant and the result is given as

$$j_{nm}(\rho) = -\frac{1}{2\pi}\frac{e\hbar}{m_e^*}\left[\frac{m}{\rho} + \frac{e}{\hbar}A_\varphi(\rho)\right]R^2(\rho). \quad (11)$$

By integrating this expression over the whole radial axis, one can calculate the current J_{nm} carried by the state with definite quantum numbers n,m. The result is given as

$$J_{nm} = \int_0^\infty j_{nm}(\rho)d\rho = -\frac{1}{2\pi}\frac{e\hbar}{m_e^*}\int_0^\infty\left(\frac{m}{\rho} + \frac{e}{\hbar}A_\varphi(\rho)\right)R^2(\rho)d\rho. \quad (12)$$

Utilizing the Hellman-Feynman theorem, one can prove that Eq. (12) is equivalent to

$$J_{nm} = -\frac{e}{h}\frac{\partial E_{nm}}{\partial m}. \quad (13)$$

When the limit of the uniform magnetic field is taken, namely, when $\rho_1 \equiv \rho_2$ and $D\to\infty$, the energy eigenvalues become

$$E^*_{nm} = n + \tfrac{1}{2}(|m| + m + 1), \quad (14)$$

and the radial wave function reduces to

$$R(\rho) = \frac{1}{r_B}\left[\frac{n!}{(n+|m|)!}\right]^{1/2}\exp\left(-\frac{1}{4}\frac{\rho^2}{r_B^2}\right)\left(\frac{1}{2}\frac{\rho^2}{r_B^2}\right)^{|m|/2} \times L_n^{|m|}\left(\frac{1}{2}\frac{\rho^2}{r_B^2}\right), \quad (15)$$

where $L_n^{(\alpha)}(x)$ is a generalized Laguerre polynomial,[24] which are the well-known Landau levels.[1] It is worthwhile to note here that the corresponding current J^*_{nm}, which is in units of $e\omega_B/2\pi$, becomes

$$J^*_{nm} = -\frac{1}{2}\left(m\frac{n!}{(n+|m|)!}\int_0^\infty e^{-x}x^{|m|-1}[L_n^{|m|}(x)]^2dx + 1\right). \quad (16)$$

Explicit evaluation yields[26]

$$J^*_{nm} = \begin{cases} 0, & m<0 \\ -\frac{1}{2}, & m=0 \\ -1, & m>0, \end{cases} \quad (17)$$

which is independent of the radial quantum number n. The vanishing current for negative m and a constant value for positive m indicate that the direction of the electron's circular motion is fixed for a chosen static magnetic field. And the nonvanishing current for the magnetic index $m=0$ results from a contribution from the vector potential: the angular momentum quantum number is not m but $m + (1/2)(eB/\hbar)\rho^2$.

III. RESULTS AND DISCUSSIONS

In this section results are presented and analyzed for the calculated energy spectra and the persistent currents for the quantum structures described in Sec. II. In doing this, we have used the dimensionless variable ρ^* and lengths ρ_i^*, $i=1,2$, and D^*, which are normalized by the magnetic radius accordingly:

$$\rho^* \equiv \frac{\rho}{r_B}, \quad \rho_i^* \equiv \frac{\rho_i}{r_B}, \quad D^* \equiv \frac{D}{r_B}. \quad (18)$$

A. Magnetically confined electrons

First, an unbounded two-dimensional electron gas is considered under nonuniform magnetic fields with the field-free region at the center, namely, when $D^*\to\infty, \rho_1^*\to 0$ in Fig. 1. The resulting energy spectra E^*_{nm} are plotted in Fig. 2 as a function of the normalized radius ρ_2^* for various m with a fixed $n=0$. It is seen that E^*_{nm} deviate from the results of uniform magnetic fields ($\rho_2^*=0$). They decrease monotonically as ρ_2^* increases. At large ρ_2^* the energies tend to those of the situation where the electron is confined in a field-free circular disk of radius ρ_2, and consequently levels with the same $|m|$ have the same energy. This tendency is clearly seen here so that energies with the same $|m|$ get closer to each other as ρ_2^* increases, and at large ρ_2^* these levels become almost degenerate. As we mentioned in the Introduction, the magnetic quantum number m in cylindrical coordinates plays a similar role to the guiding center of magnetic oscillations in Cartesian geometry (see Ref. 27). This means that the larger $|m|$ is, the further the wave function is located from the origin. Accordingly, energy levels with smaller $|m|$ deviate more from the values of the uniform magnetic field case for a given n and a fixed ρ_2^*.

In order to demonstrate the change of energy spectrum due to the presence of nonuniform magnetic fields further, E^*_{nm} are shown in Fig. 3 as a function of the magnetic quantum number m for a fixed $\rho_2^*=8$. What is seen is that such a simple geometrical perturbation of uniform magnetic fields can lead to the partial lift of the degeneracy of the bulk Landau levels. The result for the uniform field case has been given in Eq. (14). The lifted states near the origin should be distinguished from the edge states that are typically caused by an electrical potential or a confining barrier. We have also seen that this lift of degeneracy becomes more prominent for

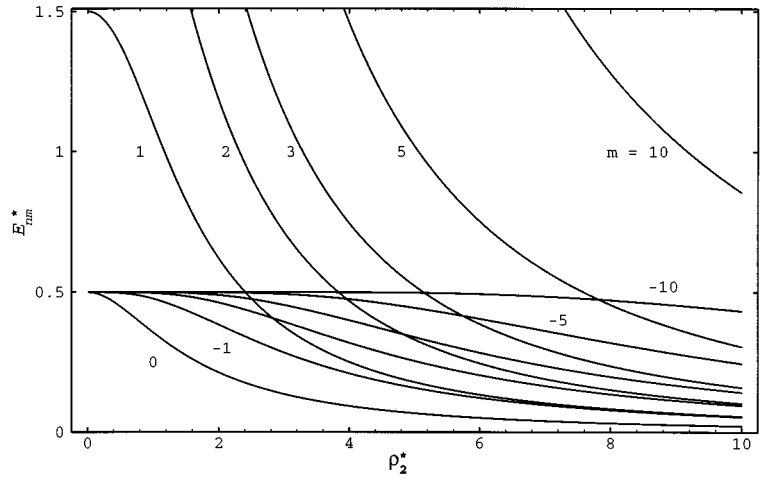

FIG. 2. Energy eigenvalues of an electron in magnetic fields with a field-free circular cavity at the center in an unbounded two-dimensional plane ($\rho_1=0$, $\rho_2\neq 0$, and $D^*=\infty$ in Fig. 1) as a function of the radius $\rho_2^*=\rho_2/r_B$ where the magnetic length $r_B=(\hbar/eB)^{1/2}$; a radial quantum number $n=0$ is chosen and the numbers near the curves denote the magnetic indices.

larger ρ_2^*, meaning that more levels deviate from the uniform field results of half-integer values. However, there always exist infinitely many degenerate levels for an unbounded system. Furthermore, an additional degeneracy emerges at large ρ_2^* as already discussed in Fig. 2, i.e., levels with the same $|m|$ have almost the same energy in the strong field limit for a chosen radius of field-free disk cavity. Note that the state of $m=0$ always has the least energy among the states for a given n. In other words, we have generated a true ground orbit by introducing a field-free region at the center: all levels with $m\leqslant 0$ were degenerate for the uniform field case.

Change of energy with m implies, according to Eq. (13), that these states carry current. In particular, some of the levels with negative m become current-carrying states. We have used Eq. (12) in order to evaluate J_{nm}^*, which is the current carried by the definite quantum state with radial quantum number n and magnetic quantum number m. Our calculations show that for non-negative m, the absolute value of the current decreases monotonically as ρ_2^* increases. On the other hand, for negative m, currents vanish identically in a uniform magnetic field, but when ρ_2^* increases from zero, currents increase up to certain points and then decrease gradually. For fixed ρ_2^* and n, the deviations of the currents J_{nm}^* from the uniform field results of Eq. (17) are smaller for larger $|m|$.

Although the structure considered is simple, we find it interesting to calculate the net equilibrium currents for the present configuration as a function of the electron numbers that are to be added into the structure by varying the gate voltage in experiments. The total current I^* at zero temperature is constructed according to

$$I^*=\sum_{n,m} J_{nm}^*\Theta(E_F^*-E_{nm}^*), \tag{19}$$

where E_F^* is the Fermi energy and Θ is the Heaviside step function. Before analyzing our data we notice that the results for the uniform magnetic fields are intriguing. All levels with nonpositive m are degenerate; however, their contribution to currents is different: J_{nm}^* is $-1/2$ for $m=0$ and 0 for $m<0$ [see Eq. (17)]. Therefore, there appears an ambiguity in determining which state is to be filled first among infinitely degenerate levels with $m\leqslant 0$ in which the $m=0$ state is the only current-carrying state. By introducing a field-free cavity this ambiguity is removed in our model, and it turns out that state $m=0$ is the lowest energy level as discussed earlier. The total current versus number of electrons N is plotted in Fig. 4 for a chosen value of $\rho_2^*=8$. It shows that the structure of the resulting current as a function of the number of electrons in the system is not trivial even for the present simple model. Hereafter, the Dirac notation $|n,m\rangle$ is used to

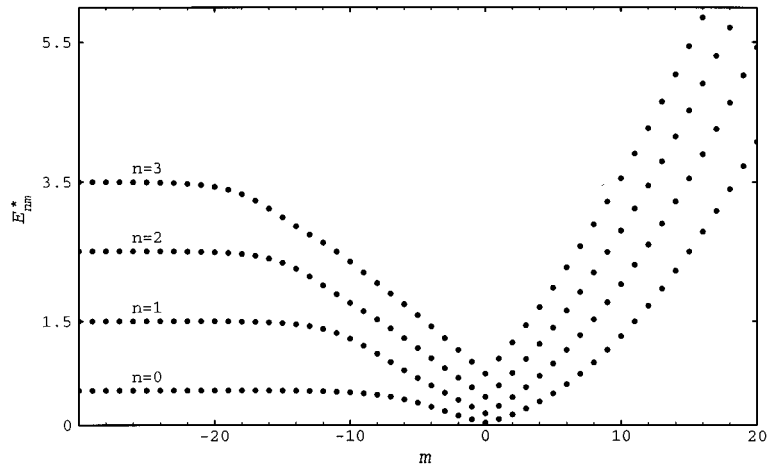

FIG. 3. Energy spectrum E_{nm}^* for the same quantum structure as considered in Fig. 2 as a function of the magnetic index m for $n=0$, 1, 2, and 3; $\rho_2^*=8$ has been chosen and energies are in units of $\hbar\omega_B$ where $\omega_B=eB/m_e^*$.

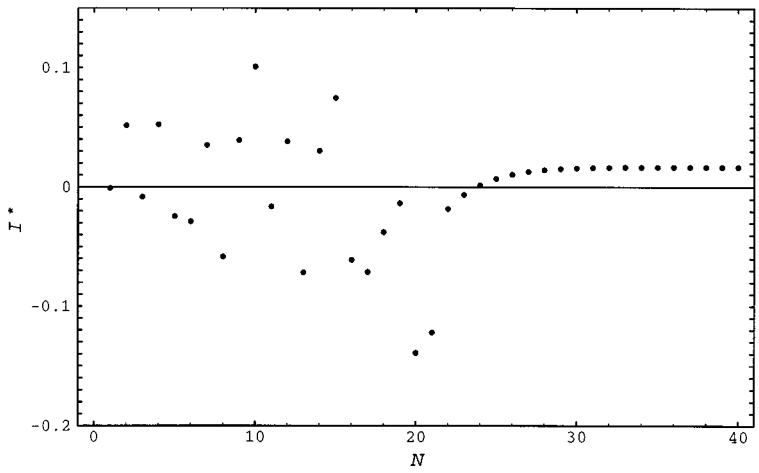

FIG. 4. Current I^* for the same structure considered in Fig. 2 as a function of the number of electrons for a fixed $\rho_2^*=8$ [see Eq. (19)] in units of $e\omega_B/2\pi$.

denote a particular state with radial quantum number n and magnetic index m. The first electron occupies $|0,0\rangle$ in Fig. 3, which gives a negligible contribution to the current. The second electron occupies the next lowest level of $|0,-1\rangle$, which results in $J^*_{0-1}\doteq 0.05$, and accordingly the net current I^* equals $J^*_{00}+J^*_{0-1}\approx J^*_{0-1}$. The next electron occupies $|0,1\rangle$, which gives rise to a contribution to the current by $J^*_{01}\doteq -0.06$, which is close to J^*_{0-1} apart from the sign, and thus the magnitude of the persistent current reduces to $I^*\doteq -0.01$. This procedure is repeated until all available electrons are used up and the resulting value is the net current. Here, one should notice that levels with $n=1$ participate also in determining the net currents since some of them lie below the Fermi energy depending on the number of electrons, as is seen in Fig. 3. Consequently, the values of current look randomly distributed until $N\sim 22$ in Fig. 4. After a certain stage adding more electrons does not affect the net current since the Fermi energy is eventually locked on the unperturbed degenerate energy levels with no contribution to currents. For a chosen ρ_2^* this saturation value of the total current is uniquely determined, and $I^*\doteq 0.017$ in Fig. 4. More levels deviate from the unperturbed half-integer values for a larger ρ_2^*. Accordingly this saturation value is achieved at a greater N.

Now, let us consider an unbounded two-dimensional electron gas under nonuniform magnetic fields with a field-free annulus region, i.e., when $D^*\to\infty$, $0<\rho_1^*<\rho_2^*$ in Fig. 1. This different spatial modulation of applying magnetic fields brings new features to the energy spectrum and, accordingly, to the behavior of the persistent current. In Fig. 5 the energy spectra E^*_{nm} are drawn as a function of ρ_1/ρ_2 for a particular magnetic index $m=0$, where $\rho_2^*=4$ and 10 were considered. What is seen is that as the ratio approaches the value 1, the energy levels restore the usual Landau levels [see Eq. (14)]. On the other hand, the results of Fig. 2 are recovered in the opposite limit of vanishing ρ_1^*. In the intermediate regime where $0<\rho_1^*/\rho_2^*<1$ the energy spectra manifest a great deal of structure. It is seen in Fig. 5(a) that the energy levels increase gradually to half-integer values, where a relatively small ρ_2^* is used. However, as ρ_2^* gets bigger, the adjacent levels interact with each other and the level repulsion occurs. The anticrossing of levels is evident in Fig. 5(b) where $\rho_2^*=10$ has been used. Since ρ_2^* has been normalized with respect to the magnetic radius r_B, a large ρ_2^* may be achieved either by increasing ρ_2 for a fixed B or by increasing the magnitude of B for a chosen ρ_2.

In Fig. 6 the energy spectra E^*_{nm} are plotted as a function of the magnetic index m for a chosen $\rho_2^*=10$ for several values of the ratio ρ_1/ρ_2. The prominent feature is the lift of degeneracy of levels, which results from the influence of nonuniform magnetic fields. It is observed that the dispersion in the energy spectrum diminishes to the usual Landau levels as the field-free region is filled out by magnetic fields, (a)→(b). Compared with the results of Fig. 3 where a field-free circular cavity was introduced in a system with otherwise uniform fields, the present result shows that an additional introduction of inner magnetic fields causes a shift of the minimum of each level to a bigger negative m. The greater ρ_1/ρ_2, the larger the shift.

The net current is depicted in Fig. 7 as a function of the electron numbers at zero temperature, where $\rho_2^*=10$ and $\rho_1/\rho_2=0.6$ have been used. This result is the outcome of adding the currents carried by the single electron orbitals up to the Fermi energy in the corresponding energy spectrum. In Fig. 6(b) the lowest level is $|0,-18\rangle$, which will be occupied by the first electron. This state contributes a negligible amount of 0.001 to the total current. The next electron will occupy the state $|0,-17\rangle$, which carries a current of $J^*_{0-17}\doteq -0.013$. Then, the sum of the two contributions gives rise to the total current in Fig. 7 for $N=2$. When another electron is in the system, it will occupy the next level of $|0,-19\rangle$, which carries a current of $J^*_{0-19}\doteq 0.014$. This alternating occupation of levels around $m=-18$ continues as one adds more electrons to the system. In Fig. 7 the net current remains unchanged at $I^*\doteq -0.06$ when $N\approx 40$ is reached. This is because levels with $m\geqslant -10$ or $m\leqslant -30$ do not carry currents. Accordingly, adding more electrons does not affect the net current. The scattered feature of the current for electron numbers $N\leqslant 40$ is due to the contribution from higher levels with $n=1$ for magnetic indices $-17\leqslant m\leqslant -13$, in which energies are less than those of levels with $n=0$ for $m\geqslant -9$ or $m\leqslant -26$. What is more interesting is the appearance of a sudden jump in the magnitude of the net current when the electron number becomes

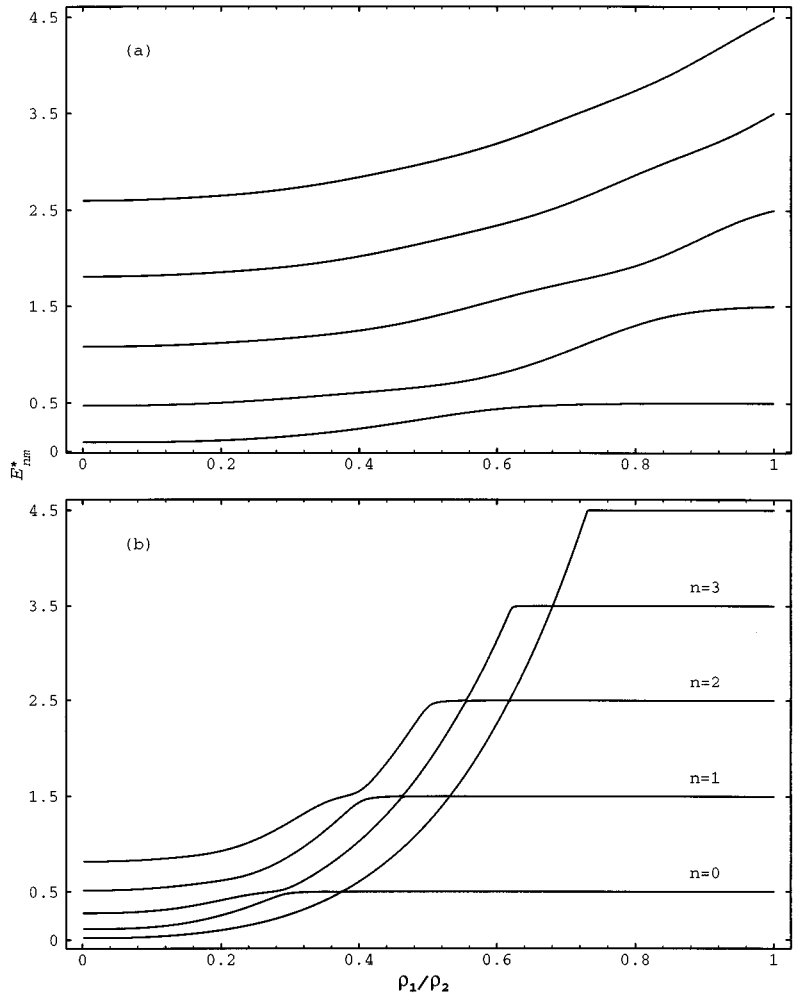

FIG. 5. Energy dispersion as a function of the ratio ρ_1/ρ_2 for the structures with field-free annulus ($\rho_1 \neq 0$, $\rho_2 \neq 0$, and $D^* = \infty$ in Fig. 1) otherwise under uniform fields; (a) $\rho_2^* = 4$ and (b) $\rho_2^* = 10$, where only one magnetic index $m = 0$ is used.

$N = 69$ and the value remains there. This jump results from the occupation of the level $|0,0\rangle$ by the 69th electron, which carries the current value of $J_{00}^* \doteq -0.5$. Then, additional electrons will occupy the levels with $n = 0$ for $m \leqslant -61$, all of which do not carry currents. They are the usual bulk Landau levels with energy of one-half.

B. Quantum disk in nonuniform magnetic fields

Lift of the degeneracy of Landau levels may be also achieved when an external electrostatic potential is superimposed on uniform magnetic fields. The problem of a quantum disk of radius D^* in the uniform magnetic field can be incorporated in our formulation by setting $\rho_1^* = \rho_2^* \equiv 0$ in Fig. 1. Landau levels of a quantum disk with an infinitely high potential barrier of $V_0^* \to \infty$ have been treated in Ref. 22. First, we report the result for the soft wall boundary condition. When the height of the potential barrier becomes finite, new features of the energy spectrum appear. The energy dispersion relation in the magnetic index is shown in Fig. 8 for $D^* = 7$ with barrier height $V_0^* = 6$, where energies with $m > 0$ are not drawn because there is no appreciable difference compared to the results of uniform magnetic fields, i.e., Eq. (14). The anticrossing and repulsion of the levels with different quantum number n are clearly seen. Comparison with the energy spectrum for a similar configuration in Cartesian geometry[4] suggests that the magnetic quantum number m plays a similar role as the center of magnetic oscillations does in rectangular coordinates. The levels near $m = 0$ remain in the bulk Landau levels. This is due to the fact that wave functions are mostly localized near the origin of the quantum dot, so that they do not feel the influence of the outer boundary. The flat dispersion in the energy spectrum for large negative m regardless of n reflects the fact that the corresponding wave packets of those levels are mainly located outside the quantum dot. Accordingly the energy eigenvalues appear as $\sim(n + \frac{1}{2}) + V_0^*$. The levels located in the dispersed parts of the energy curves are edge states, which represent electron wave functions strongly influenced by the electrostatic boundary. These edge states carry currents.

Now, let us consider quantum dot problems ($V_0^* = \infty$) under nonuniform magnetic fields. We first take the configuration such that $\rho_1^* = 0$ and $D^* = 14$ in Fig. 1. The superposition of two influences, one from the hard wall confinement and the other one due to the nonuniformity of the applied magnetic fields, leads to the energy spectrum demonstrated in Fig. 9. The hard wall boundary condition gives rise to the edge states for large negative m. And the effect of the field-free cavity causes the lift of the degeneracy of the bulk Landau levels near $m = 0$. This lift of degeneracy becomes more

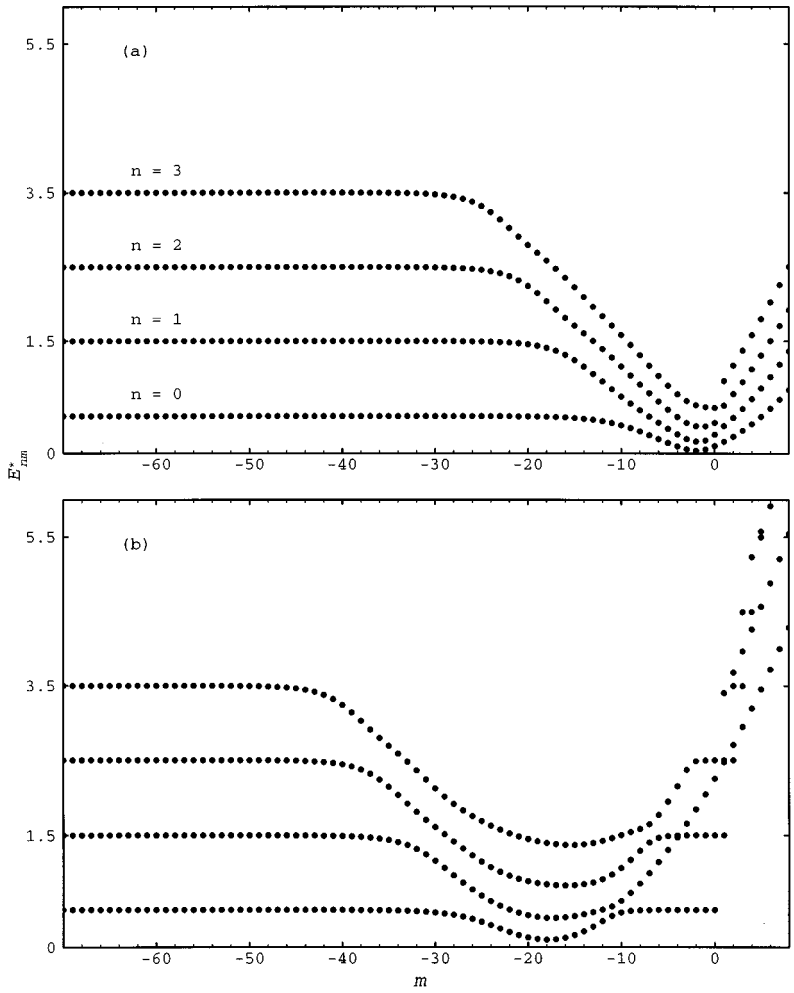

FIG. 6. Energy spectra E^*_{nm} as a function of the magnetic index m for structures described in Fig. 5 where $\rho_2^*=10$ is used: (a) $\rho_1/\rho_2=0.2$; (b) $\rho_1/\rho_2=0.6$.

evident as ρ_2^* increases. For instance, when $\rho_2^*=4$ in Fig. 9(a), many levels in the bulk remain dispersionless with respect to changes of the magnetic index. However, as ρ_2^* increases to 10, a great deal of dispersion appears in Fig. 9(b). The limit of $\rho_2^*\rightarrow D^*$ corresponds to the situation where free particles are confined in a circular disk.

In Fig. 10 the persistent currents are drawn for the present structure as a function of electron numbers. It has been reported that for the quantum dot in uniform magnetic fields this dependence of the equilibrium current on the electron number has the characteristic behavior of possessing flat parts that alternate with regions of sudden jumps in magnitude.[22] The same structure is seen in Fig. 10(a), where $\rho_2^*=0$ was used in order to represent the quantum disk of radius D^* under uniform perpendicular magnetic fields. The pronounced current plateaus that are seen are consequences

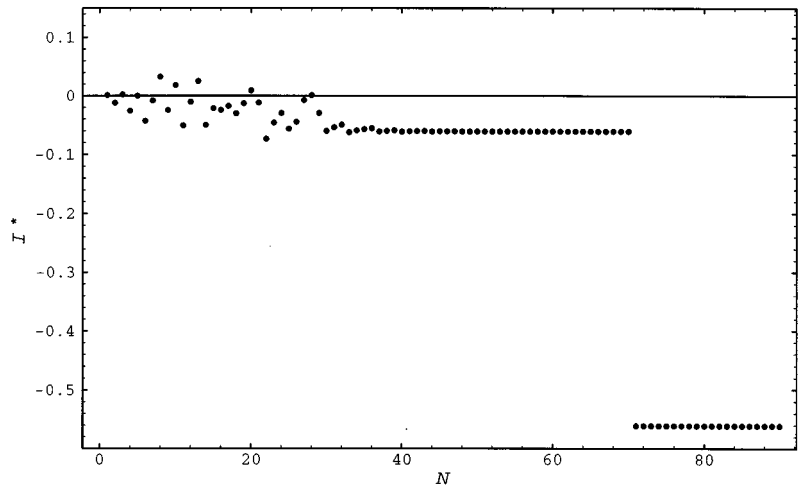

FIG. 7. Total current for the same structure considered in Fig. 5 as a function of the number of electrons N for $\rho_2^*=10$ and $\rho_1^*/\rho_2^*=0.6$.

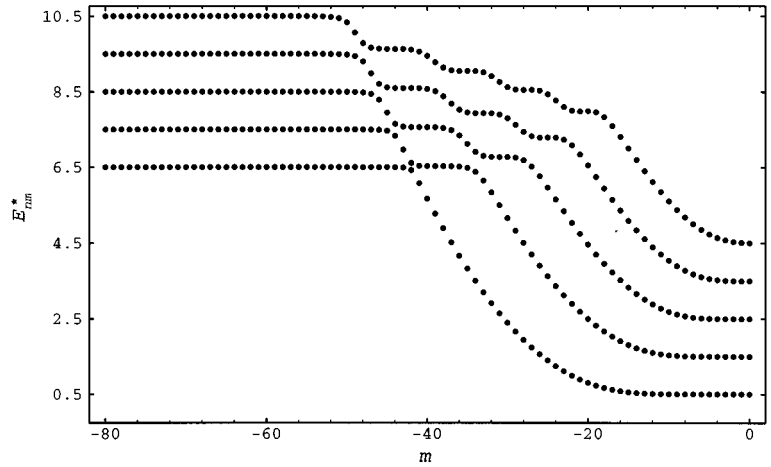

FIG. 8. Energy spectrum of a quantum disk with $D^*=7$ and $V_0^*=6$ as a function of the magnetic index m.

of electrons occupying non-current-carrying bulk Landau levels. Accordingly, the difference in the value of current between two adjacent plateaus is observed to be one-half. The shooting branch of the current curve as electron numbers increase is due to the contribution from the edge states. Sudden drops take place whenever an electron occupies a Landau level with the magnetic index $m \geqslant 0$. The results in Figs. 10(b) – 10(d) are obtained after introducing the field-free cavity: $\rho_2^*=4$, 6, and 8 are used respectively. For a relatively small ρ_2^*, i.e., Fig. 10(b), the current quantization as a function of electron number is still seen. However, the values of the current at each plateau are different from the uniform field result. This is because of the contribution from the lifted Landau levels to the current in the bulk. Also, it is worth noticing that the value of current at a plateau might be positive, while for a quantum disk in a uniform magnetic field the quantized values are always negative as is obvious in Fig. 10(a). As the perturbation of uniform magnetic field increases, the characteristic behavior of current quantization in uniform magnetic fields will be destroyed. This is seen in Figs. 10(b)–10(d), where the length of the plateau decreases with increasing ρ_2^*, and at large ρ_2^* the irregular structure of the persistent current is observed.

Finally, the most general form that is depicted in Fig. 1 is considered. The chosen parameters are $D^*=14$, $\rho_2^*=10$, and inner radius ρ_1^* is varied. In Fig. 11 a typical single-particle energy spectrum is shown for the ratio $\rho_1/\rho_2=0.6$. Similar features to Fig. 9 are seen: edge states are apparent for large negative m and degenerate Landau levels are lifted in the bulk due to the perturbation of uniform magnetic fields by imposing an annulus field-free region. It is interesting to note again the shift of the lowest energy level toward a larger negative m. Compared to the results from an unbounded structure under the same magnetic modulation (Fig. 6), the difference is in the lift of degenerate levels with large negative m due to the effect of the infinite potential barrier.

The persistent currents associated with the present quantum structure are also evaluated at zero temperature. The results are given in Fig. 12 where several values of ρ_1/ρ_2 are used to demonstrate a variety of features. It is seen that at small values of ρ_1/ρ_2 the resulting currents look random in electron number [Fig. 12(a)]. However, increasing the ratio ρ_1/ρ_2 [Figs. 12(b) – 12(d)] leads to a more regular structure. For instance, the transit from Fig. 12(b) to Fig. 12(d) clearly shows how the plateaus in the $I-N$ characteristic are formed. It is evident that introducing an annulus-field free cavity inside a quantum dot washes out the current plateaus. As the degree of nonuniformity increases the current quantization as a function of N disappears. One of the noticeable differences in the obtained persistent currents between a quantum dot in a uniform magnetic field [see Fig. 10(a)] and one under nonuniform magnetic fields [Figs. 12(c)–12(d)] is the fact that the value of the current on the first plateau equals negative one-half for the former case but is nearly zero for the latter. This is due to the fact that for the case of uniform magnetic fields the quantum state with $m=0$ has the least energy compared to other levels with negative m. Accordingly, it will be occupied by the first electron, which contributes a value of $-1/2$ to the current. However, in the case of a quantum dot under nonuniform magnetic fields the energy of states with negative m can be less than that with the level of $m=0$ (see Fig. 11). Therefore, electrons will first occupy those states that make negligible contributions to the current before filling in the $m=0$ orbital, which will be occupied only at sufficiently large N.

IV. CONCLUDING REMARKS

We have considered an independent electron gas confined in one direction under the influence of spatially modulated magnetic fields applied perpendicular to the system within an effective-mass approximation. Consequently, single-particle energy spectra were obtained and used to determine the relevant azimuthal currents carried by definite quantum states. Anticrossing and the repulsion of Landau levels were observed when an annulus perturbation was introduced in otherwise uniform magnetic fields as a function of the ratio of the inner and outer radii of the field-free annula. One prominent feature of our results is that the degeneracy of the bulk Landau levels can be lifted by this simple geometrical perturbation of the applied magnetic fields. These lifted states carry currents that are to be distinguished from edge states that typically result from a potential barrier. Accordingly, we have demonstrated that the net equilibrium azimuthal current may not vanish even for an unbounded two-dimensional electron gas, but rather saturates to a finite value unlike the uniform magnetic field case.

In addition, quantum dot problems have been treated by imposing an electrostatic potential wall on the two-dimensional electron gas in the strong magnetic field limit. In this case, the pronounced edge states near the boundary played an important role in determining the Fermi energy of the system and thus in obtaining the persistent currents. We have shown that a simple spatial modulation of the applied magnetic fields in quantum dots gives rise to noticeable changes in the energy spectrum and consequently in persistent currents. This subject is of particular interest now since it has become possible to fabricate magnetic quantum disks using nanolithographic techniques.[20]

An experimental realization of our model structure may be achieved by depositing an annular area of magnetic or superconducting material on top of a two-dimensional electron gas, say on the surface of $GaAs/Al_xGa_{1-x}As$ heterostructures. Periodic spatial modulation of magnetic fields has already been realized in strip geometry by several experimental groups.[16,18,19]

In our calculation neither electron-electron scattering nor disorder was considered. However it has been reported in a recent work that the effect of the Coulomb interaction on persistent currents is negligible in clean mesoscopic rings.[28] It has also been argued that the plateau structure of persistent current [see Fig. 10(a)] survives against weak disorder for a similar simply connected system of quantum disks.[22]

Recently, theoretical analyses of the quantum structures created by nonhomogeneous magnetic fields in Cartesian geometry have been made.[29,30] It has been demonstrated that increasing the number of magnetic strips and alternating them with field-free regions yields a variety of rich electronic and transport properties. We expect that similar physical effects will be obtained in the configuration discussed in this paper by forming cylindrical lateral magnetic superlattices.

Finally, we want to mention that the Aharonov-Bohm flux Φ (Ref. 31) pierced at the origin can be included in our model. By a straightforward calculation it can be shown that one has only to replace the magnetic quantum number m by $m+\Phi/\Phi_0$ in the formulas derived in Sec. II for this goal, where $\Phi_0=h/e$ is the magnetic flux quantum. Also, it can be proved that the following equation holds because of the gauge invariance:

$$E^*_{n,m}(\Phi/\Phi_0+1)=E^*_{n,m+1}(\Phi/\Phi_0). \tag{20}$$

A thorough discussion of the role of this flux in regard to detecting currents J^*_{nm} can be found in Ref. 21. The same arguments can be applied to our case as well. Since the specific value of Φ is immaterial in the evaluation of the current, only the results for $\Phi=0$ have been presented in our work.

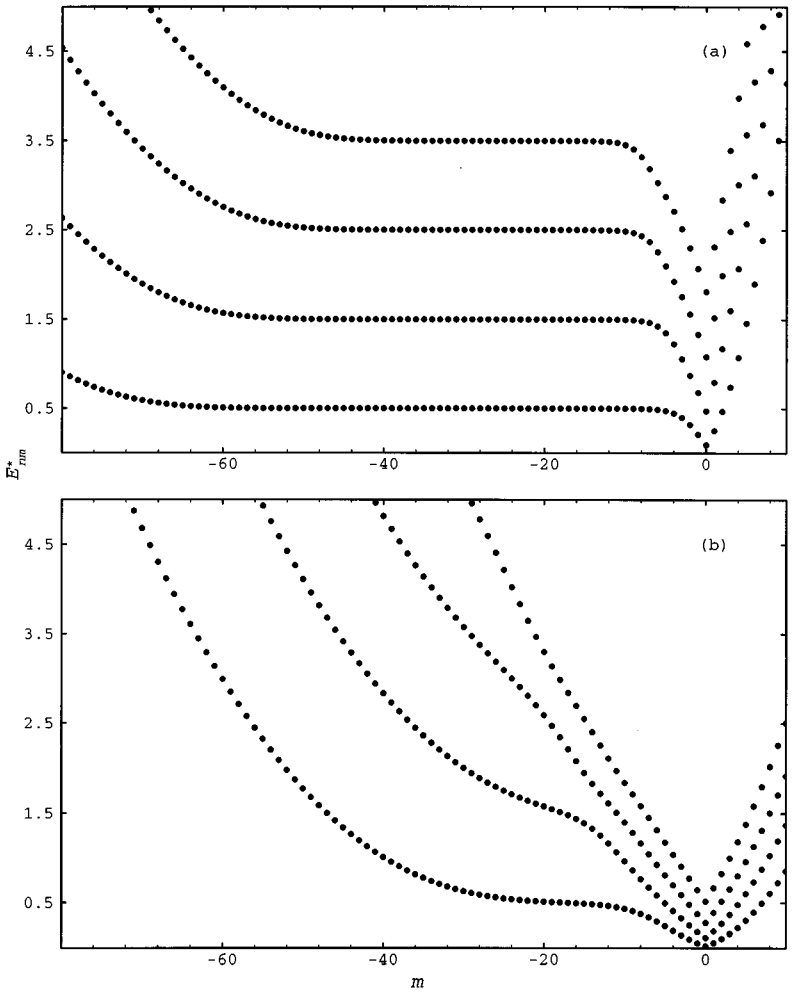

FIG. 9. Energy spectra E^*_{nm} of a quantum dot with a field-free circular cavity at center otherwise under perpendicular uniform magnetic fields ($\rho_1=0$, $\rho_2\neq 0$, and $D^*=14$): (a) $\rho_2^*=4$ and (b) $\rho_2^*=10$.

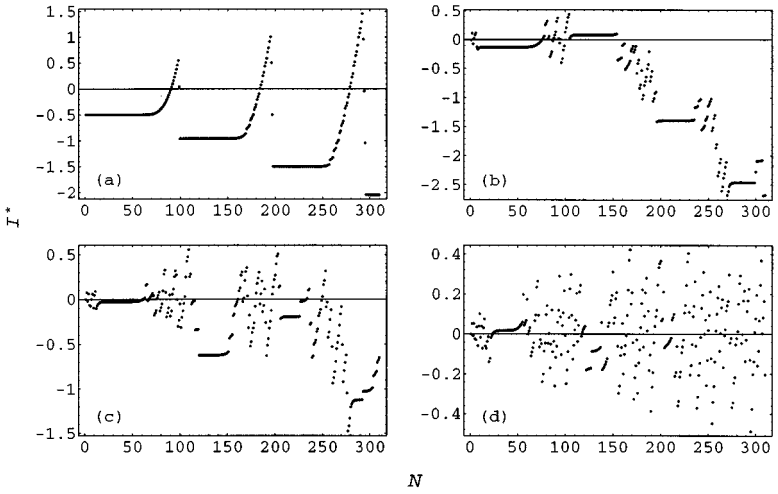

FIG. 10. Persistent currents I^* associated with the same structure considered in Fig. 9 as a function of the number of electrons where (a) $\rho_2^*=0$, (b) $\rho_2^*=4$, (c) $\rho_2^*=6$, and (d) $\rho_2^*=8$.

ACKNOWLEDGMENTS

This work has been supported by the Ministry of Education of Korea through the Basic Sciences Research Institute at CNU (Grant No. BSRI-95-2431).

APPENDIX

The transcendental equation that we have used in determining the energy spectrum for the structure depicted in Fig. 1 is given as

$$\det\begin{pmatrix} G_{11} & G_{12} & G_{13} & 0 & 0 & 0 \\ G_{21} & G_{22} & G_{23} & 0 & 0 & 0 \\ 0 & G_{32} & G_{33} & G_{34} & G_{35} & 0 \\ 0 & G_{42} & G_{43} & G_{44} & G_{45} & 0 \\ 0 & 0 & 0 & G_{54} & G_{55} & G_{56} \\ 0 & 0 & 0 & G_{64} & G_{65} & G_{66} \end{pmatrix}=0, \quad \text{(A1)}$$

where the nonzero matrix elements are specified to be

$$G_{11}=M\left(\frac{1+m+|m|}{2}-E^*,|m|+1,\frac{1}{2}\rho_1^{*2}\right)\exp\left(-\frac{1}{4}\rho_1^{*2}\right)\times\left(\frac{1}{2}\rho_1^{*2}\right)^{|m|/2}, \quad \text{(A2)}$$

$$G_{12}=-J_{|m+(1/2)\rho_1^{*2}|}(2^{1/2}E^{*1/2}\rho_1^*), \quad \text{(A3)}$$

$$G_{13}=-Y_{|m+(1/2)\rho_1^{*2}|}(2^{1/2}E^{*1/2}\rho_1^*), \quad \text{(A4)}$$

$$G_{21}=\rho_1^*\left[\left(-\frac{1}{2}+\frac{|m|}{\rho_1^{*2}}\right)M\left(\frac{1+m+|m|}{2}-E^*,|m|+1,\frac{1}{2}\rho_1^{*2}\right)+M'\left(\frac{1+m+|m|}{2}-E^*,|m|+1,\frac{1}{2}\rho_1^{*2}\right)\right]\times\exp\left(-\frac{1}{4}\rho_1^{*2}\right)\left(\frac{1}{2}\rho_1^{*2}\right)^{|m|/2}, \quad \text{(A5)}$$

$$G_{22}=-2^{1/2}E^{*1/2}J'_{|m+(1/2)\rho_1^{*2}|}(2^{1/2}E^{*1/2}\rho_1^*), \quad \text{(A6)}$$

$$G_{23}=-2^{1/2}E^{*1/2}Y'_{|m+(1/2)\rho_1^{*2}|}(2^{1/2}E^{*1/2}\rho_1^*), \quad \text{(A7)}$$

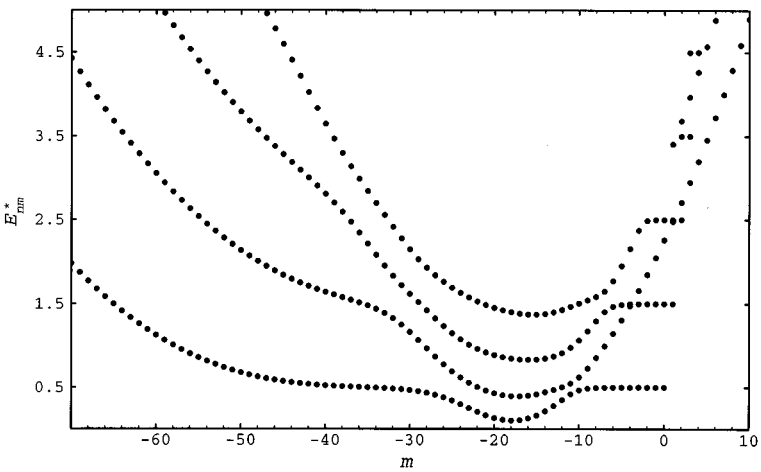

FIG. 11. Single-particle energy spectrum E^*_{nm} for the quantum dots described in Fig. 1 with $D^*=14$; $\rho_2^*=10$ and $\rho_1/\rho_2=0.6$ are chosen.

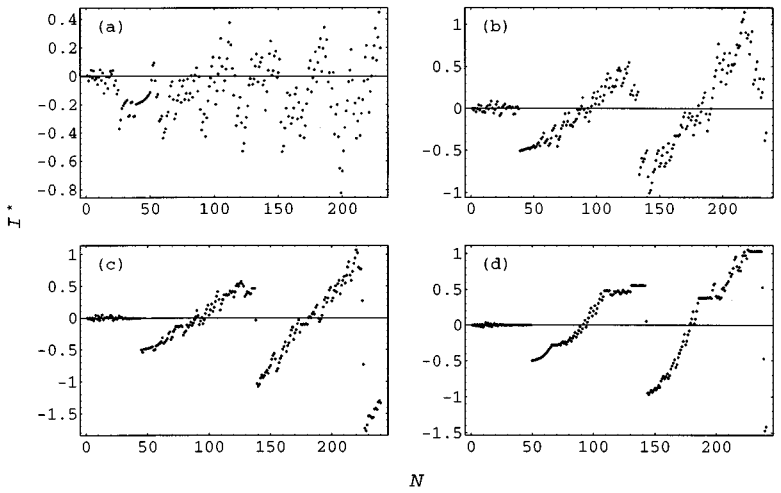

FIG. 12. Associated persistent currents I^* with the same quantum structure considered in Fig. 11 ($D^*=14$) as a function of the number of electrons: (a) $\rho_1/\rho_2=0.2$, (b) $\rho_1/\rho_2=0.4$, (c) $\rho_1/\rho_2=0.6$, (d) $\rho_1/\rho_2=0.8$, where $\rho_2^*=10$ is used.

$$G_{32}=J_{|m+(1/2)\rho_1^{*2}|}(2^{1/2}E^{*1/2}\rho_2^*), \tag{A8}$$

$$G_{33}=Y_{|m+(1/2)\rho_1^{*2}|}(2^{1/2}E^{*1/2}\rho_2^*), \tag{A9}$$

$$G_{34}=-U\left(\alpha-E^*,\beta,\frac{1}{2}\rho_2^{*2}\right)\exp\left(-\frac{1}{4}\rho_2^{*2}\right)\left(\frac{1}{2}\rho_2^{*2}\right)^{\gamma}, \tag{A10}$$

$$G_{35}=-M\left(\alpha-E^*,\beta,\frac{1}{2}\rho_2^{*2}\right)\exp\left(-\frac{1}{4}\rho_2^{*2}\right)\left(\frac{1}{2}\rho_2^{*2}\right)^{\gamma}, \tag{A11}$$

$$G_{42}=2^{1/2}E^{*1/2}J'_{|m+(1/2)\,\rho_1^{*2}|}(2^{1/2}E^{*1/2}\rho_2^*), \tag{A12}$$

$$G_{43}=2^{1/2}E^{*1/2}Y'_{|m+(1/2)\,\rho_1^{*2}|}(2^{1/2}E^{*1/2}\rho_2^*), \tag{A13}$$

$$G_{44}=-\rho_2^*\left[\left(-\frac{1}{2}+\frac{2\gamma}{\rho_2^{*2}}\right)U\left(\alpha-E^*,\beta,\frac{1}{2}\rho_2^{*2}\right)+U'\left(\alpha-E^*,\beta,\frac{1}{2}\rho_2^{*2}\right)\right]\exp\left(-\frac{1}{4}\rho_2^{*2}\right)\left(\frac{1}{2}\rho_2^{*2}\right)^{\gamma}, \tag{A14}$$

$$G_{45}=-\rho_2^*\left[\left(-\frac{1}{2}+\frac{2\gamma}{\rho_2^{*2}}\right)M\left(\alpha-E^*,\beta,\frac{1}{2}\rho_2^{*2}\right)+M'\left(\alpha-E^*,\beta,\frac{1}{2}\rho_2^{*2}\right)\right]\exp\left(-\frac{1}{4}\rho_2^{*2}\right)\left(\frac{1}{2}\rho_2^{*2}\right)^{\gamma}, \tag{A15}$$

$$G_{54}=U\left(\alpha-E^*,\beta,\frac{1}{2}D^{*2}\right), \tag{A16}$$

$$G_{55}=M\left(\alpha-E^*,\beta,\frac{1}{2}D^{*2}\right), \tag{A17}$$

$$G_{56}=-U\left(\alpha-(E^*-V_0^*),\beta,\frac{1}{2}D^{*2}\right), \tag{A18}$$

$$G_{64}=\left(-\frac{1}{2}+\frac{2\gamma}{D^{*2}}\right)U\left(\alpha-E^*,\beta,\frac{1}{2}D^{*2}\right)+U'\left(\alpha-E^*,\beta,\frac{1}{2}D^{*2}\right), \tag{A19}$$

$$G_{65}=\left(-\frac{1}{2}+\frac{2\gamma}{D^{*2}}\right)M\left(\alpha-E^*,\beta,\frac{1}{2}D^{*2}\right)+M'\left(\alpha-E^*,\beta,\frac{1}{2}D^{*2}\right), \tag{A20}$$

$$G_{66}=-\left[\left(-\frac{1}{2}+\frac{2\gamma}{D^{*2}}\right)U\left(\alpha-(E^*-V_0^*),\beta,\frac{1}{2}D^{*2}\right)+U'\left(\alpha-(E^*-V_0^*),\beta,\frac{1}{2}D^{*2}\right)\right], \tag{A21}$$

where the primes appearing on top of $J_\nu(x)$, $Y_\nu(x)$, $M(a,b,x)$, and $U(a,b,x)$ denote the derivative with respect to x. Note that all physical variables are written in terms of the dimensionless forms introduced in Eqs. (9) and (18).

[1] See, for instance, L. D. Landau and E. M. Lifshitz, *Quantum Mechanics (Non-Relativistic Theory)* (Pergamon, New York, 1977).

[2] C. Weisbuch and B. Vinter, *Quantum Semiconductor Structures* (Academic, New York, 1991).

[3] J. P. Vigneron and M. Ausloos, Phys. Rev. B **18**, 1464 (1978).

[4] E. A. Johnson, A. MacKinnon, and C. J. Goebel, J. Phys. C **20**, L521 (1987).

[5] E. A. Johnson and A. MacKinnon, J. Phys. C **21**, 3091 (1988).

[6] F. Ancilotto, A. Selloni, L. F. Xu, and E. Tosatti, Phys. Rev. B **39**, 8322 (1989).

[7] T. - L. Ho, Phys. Rev. B **50**, 4524 (1994).

[8] J. M. Ferreyra and C. R. Proetto, J. Phys. Condens. Matter **6**, 6623 (1994).
[9] O. Olendski, J. Phys. Condens. Matter **7**, 5067 (1995).
[10] C. S. Kim and O. Olendski (unpublished).
[11] D. P. Xue and G. Xiao, Phys. Rev B **45**, 5986 (1992).
[12] F. M. Peeters and P. Vasilopoulos, Phys. Rev B **47**, 1466 (1993).
[13] R. Yagi and Y. Iye, J. Phys. Soc. Jpn. **62**, 1279 (1993).
[14] C. L. Foden, M. L. Leadbeater, J. H. Burroughes, and M. Pepper, J. Phys. Condens. Matter **6**, L127 (1994).
[15] M. C. Chang and Q. Niu, Phys. Rev B **50**, 10 843 (1994).
[16] S. Izawa, S. Katsumoto, A. Endo, and Y. Iye, J. Phys. Soc. Jpn. **64**, 706 (1995).
[17] M. L. Leadbeater, C. L. Foden, T. M. Burke, J. H. Burroughes, M. P. Grimshaw, D. A. Ritchie, L. L. Wang, and M. Pepper, J. Phys. Condens. Matter **7**, L307 (1995).
[18] H. A. Carmona, A. K. Geim, A. Nogaret, P. C. Main, T. J. Foster, M. Henini, S. P. Beaumont, and M. G. Blamire, Phys. Rev. Lett. **74**, 3009 (1995).
[19] P. D. Ye, D. Weiss, R. P. Gerhadts, M. Seeger, K. von Klitzing, K. Eberl, and H. Nickel, Phys. Rev. Lett. **74**, 3013 (1995).
[20] P. D. Ye, D. Weiss, K. von Klitzing, K. Eberl, and H. Nickel, Appl. Phys. Lett. **64**, 1441 (1995).
[21] Y. Avishai, Y. Hatsugai, and M. Kohmoto, Phys. Rev. B **47**, 9501 (1993).
[22] Y. Avishai and M. Kohmoto, Phys. Rev. Lett. **71**, 279 (1993).
[23] L. Solimany and B. Kramer, Solid State Commun. **96**, 471 (1995).
[24] *Handbook of Mathematical Functions*, edited by M. Abramowitz and I. A. Stegun (Dover, New York, 1965).
[25] *Quantum Mechanics (Nonrelativistic Theory)* (Ref. 1), Sec. 115.
[26] A. P. Prudnikov, Yu. A. Brychkov, and O. I. Marichev, *Integrals and Series* (Gordon and Breach, New York, 1986), Vol. 2.
[27] B. I. Halperin, Phys. Rev. B **25**, 2185 (1982).
[28] Y. Avishai and G. Braverman, Phys. Rev. B **52**, 12 135 (1995).
[29] F. M. Peeters and A. Matulis, Phys. Rev. B **48**, 15 166 (1993).
[30] A. Matulis, F. M. Peeters, and P. Vasilopoulos, Phys. Rev. Lett. **72**, 1518 (1994).
[31] Y. Aharonov and D. Bohm, Phys. Rev. **115**, 485 (1959).